scientific reports

Check for updates

OPEN

Biochemical and structural improvements in ileum and colon with concurrent gut microbiota enhancement through intermittent fasting plasma infusions

Murat Tan[1], Taha Ceylani[2,3]✉, Rafig Gurbanov[4,5], Seda Keskin[6], Eda Acikgoz[6,7], Emrah Sağır[8] & Hikmet Taner Teker[9]✉

This study investigated the impact of intermittent fasting (IF) on older rats by administering plasma from 12-month-old male Sprague Dawley rats subjected to 35 days of IF, with 18-hour fasting intervals followed by 6-hour feeding periods. Over this period, 0.5 ml of plasma was transferred bi-daily to 24-month-old male rats, totaling 15 infusions. Infrared spectroscopy-based qualitative and quantitative analyses revealed significant changes in lipid, protein, and nucleic acid profiles, varying by tissue type and fasting regimen. Histological examination showed structural enhancements in the ileum and colon, along with reduced inflammatory markers TNF-α and COX-2, particularly with IF plasma. Additionally, plasma transfer markedly improved gut microbiota composition, increasing alpha diversity and adjusting the Firmicutes to Bacteroidetes ratio. High-Performance Liquid Chromatography results indicated elevated levels of key cecal short-chain fatty acids, suggesting enhanced gut health. These findings highlight the potential of plasma from intermittently fasting rats in modulating biomolecular profiles, intestinal tissue structure, gut microbiota, and SCFA production, offering integrated insights into intestinal health improvements.

Keywords Intermittent fasting, Plasma exchange, Intestinal tissue, Gut microbiota, TNF-α, COX-2

The gut microbiota constitutes a complex ecosystem comprising approximately 10^{13}–10^{14} microorganisms, playing essential roles in host immune regulation, nutrient fermentation, short-chain fatty acid (SCFA) production, and the maintenance of intestinal epithelial integrity[1–3]. Notably, SCFAs such as acetate, propionate, and butyrate serve as primary energy sources for colonic epithelial cells. They also enhance intestinal barrier function by promoting the expression of tight junction proteins, including claudin and occludin, and modulate inflammatory responses[4,5]. With advancing age, a reduction in microbiota diversity (loss of alpha diversity) and alterations in the Firmicutes to Bacteroidetes ratio compromise intestinal barrier integrity, leading to increased systemic inflammation[6,7]. In this context, the reciprocal interactions between intestinal tissue integrity and microbial composition are critically important, particularly in elucidating the pathophysiology of aging at the ileum and colon levels.

Recent studies have indicated that blood plasma derived from young individuals may exert rejuvenating effects on aged tissues[8,9]. The administration of young plasma to elderly animals via heterochronic plasma transfer has resulted in notable reductions in various aging markers, including hepatic fibrosis, testicular epigenetic abnormalities, and neuroinflammation[10–13]. However, the impact on the gut microbiota remains incompletely understood. Our recent study demonstrated that the administration of young plasma to aged rats

[1]Department of General Surgery, Istanbul Demiroglu Bilim University, Istanbul, Turkey. [2]Department of Molecular Biology and Genetics, Muş Alparslan University, Muş, Turkey. [3]Department of Food Quality Control and Analysis, Muş Alparslan University, Muş, Turkey. [4]Department of Bioengineering, Bilecik Şeyh Edebali University, Bilecik, Turkey. [5]Central Research Laboratory, Bilecik Seyh Edebali University, Bilecik, Turkey. [6]Department of Histology and Embryology, Van Yuzuncu Yil University, Van, Turkey. [7]Department of Neuroscience, Van Yuzuncu Yil University, Van, Turkey. [8]Department of Biology, Osmaniye Korkut Ata University, Osmaniye, Turkey. [9]Department of Medical Biology and Genetics, Ankara Medipol University, Ankara, Turkey. ✉email: t.ceylani@alparslan.edu.tr; h.tanerteker@gmail.com

enhanced gut microbiota diversity, balanced the Firmicutes/Bacteroidetes ratio, and facilitated a shift towards a youthful microbial profile[14]. In the same study, it was observed that aged plasma induced a shift in the young microbiota towards an aged profile[14]. These findings suggest that circulating factors may influence not only the biochemical properties of target tissues but also the species composition of the microbiota. Similarly, another investigation focusing on the ileum and colon reported that young plasma exhibited restorative effects at both the tissue and molecular levels in aged rats[15].

Intermittent fasting is a dietary strategy characterized by fasting intervals ranging from 16 to 24 h, which supports metabolic health and demonstrates anti-aging properties[16,17]. IF practices induce cellular autophagy, initiating tissue reconstructive processes, reducing oxidative stress levels, and suppressing inflammatory signal pathways[18]. Our previous study revealed that daily fasting cycles of 18 h significantly influenced gut microbiota composition, resulting in notable improvements in alpha diversity indices[19]. Indeed, our recent study demonstrated that IF reduces inflammation in elderly rats by increasing cellular density in the ileum and colon tissues and leads to significant decreases in the expression levels of inflammatory markers such as TNF-α and NF-κB[20]. These findings suggest that IF can modulate not only metabolic pathways[21] but also microbial composition, thereby affecting plasma composition through this mechanism[22]. In this context, the transfer of plasma obtained from individuals practicing IF to aged tissues may produce restorative effects both directly and indirectly via microbiota-mediated pathways.

In this study, we evaluated the effects of plasma derived from 12-month-old rats subjected to intermittent fasting on the integrity of ileum and colon tissues, microbiota composition, and SCFA levels in aged rats, utilizing multidisciplinary methodologies. By integrating Fourier Transform Infrared (FTIR) spectroscopy, metagenomic analyses, and high-performance liquid chromatography (HPLC) techniques, we examined the impact of plasma exchange on biomolecular profiles and the microbial ecosystem in a comprehensive manner. Additionally, we quantitatively assessed degenerative changes in tissue architecture, cellular density, and inflammatory infiltration through histological analyses. Our hypothesis posits that plasma obtained post-intermittent fasting will demonstrate rejuvenating effects on aged intestinal tissues at structural, microbial, and metabolite levels. This approach offers novel insights into the reprogram ability of circulating factors in anti-aging strategies and may provide significant indications regarding the reversibility of age-related intestinal dysfunctions.

Results

Spectrochemical analyses

Plasma applications caused significant changes in ileum and colon biomolecules

Significant qualitative changes were identified through Linear Discriminant Analysis (LDA) with 100% accuracy for all biomolecules in the ileum (Fig. 1A, Tables S1-S2). In the discrimination plot, the data from the control group (Cnt), the normal blood plasma from rats without any treatment (Npls), and the plasma from rats subjected to intermittent fasting (IFpls) clustered into distinct coordinates (Fig. 1A). The separate clustering of IFpls and Npls compared to the control indicates the impact of intermittent fasting on the plasma. Similar qualitative changes were also observed for lipids, proteins, and nucleic acids with accuracy ranging from 97% to 100% (Figs. S1-S3, Tables S3-S8). Qualitative analyses revealed identical patterns in the colon tissues, with all biomolecular profiles showing high accuracy (100%) similar to those observed in the ileum (Fig. 1B, Tables S9-S10). Like the ileum, the Npls and IFpls data clustered separately from the control group in the colon, but these clusters were closer to the control compared to the ileum. After Npls transfer, the colon tissue exhibited a profile more similar to the control compared to IFpls. Consistent differentiation was also observed for lipids, proteins, and nucleic acids with accuracy ranging between 99% and 100% (Figs. S4- S6, Tables S11-S16).

According to Beer's Lambert law, the absorption band intensity in FTIR spectra correlates with biomolecule concentrations, guiding our analysis of lipid, protein, and nucleic acid changes in the ileum and colon following plasma exchange[23]. Significant spectrochemical shifts were noted; acyl chain length (A_{2924}/A_{2962}) and triglycerides ($A_{1740}/A_{2924+2962}$) increased only after Npls transfer, evident from the lipid profile changes (Fig. 2A and B). Meanwhile, protein carbonylation showed a decrease under IFpls but rose significantly with Npls (Fig. 2C), with similar trends in protein concentration and conformation, notably higher in the Npls group (Fig. 2D and E). Protein phosphorylation and nucleic acid/protein content ratios (A_{1239}/A_{2962} and $A_{1239+1080}/A_{1653+1545}$) also increased significantly post-Npls (Fig. 2F and G). Additionally, glycogen/phosphate content was higher in the IFpls group compared to others (Fig. 2H), and glucose/protein content notably rose after Npls transfer compared to the control (Fig. 2I), underlining distinct metabolic adjustments.

In colon tissue samples, the acyl chain length ratio (A_{2924}/A_{2962}) showed no significant change between control and IFpls groups but increased with Npls (Fig. 3A). Triglyceride levels ($A_{1740/A2924+2962}$) rose, especially under IFpls compared to control (Fig. 3B). Protein carbonylation (A_{1740}/A_{1545}) decreased with IFpls and remained unchanged with Npls (Fig. 3C). Lipid concentration ($A_{2962}/A_{2962+A2924}$) significantly dropped post-IFpls (Fig. 3D). Both treatments boosted protein phosphorylation (A_{1080}/A_{1545}) compared to control (Fig. 3E). Glycogen/phosphate (A_{1050}/A_{1080}) and glucose/protein contents ($A_{1030}/A_{1653+1545}$) were higher in plasma groups, particularly under IFpls (Fig. 3F and G**).** Finally, total glycogen ($A_{1160+A1050+}A_{1031}$) was significantly elevated after IFpls alone (Fig. 3H).

Histopathological analyses

Histopathological changes in the non-fasting plasma and intermittent fasting plasma recipient rats' ileum and colon

A general morphological analysis was facilitated by the histological examination of H&E-stained sections from both the ileum and colon. In the control, there was shedding observed from the mucosal epithelial cells in both the ileum and colon, leading to the exposure of the lamina propria of the intestinal mucosa, as illustrated in Fig. 4A. In contrast, the group that received Npls plasma showed a well-structured ileum and colon. The mucosal

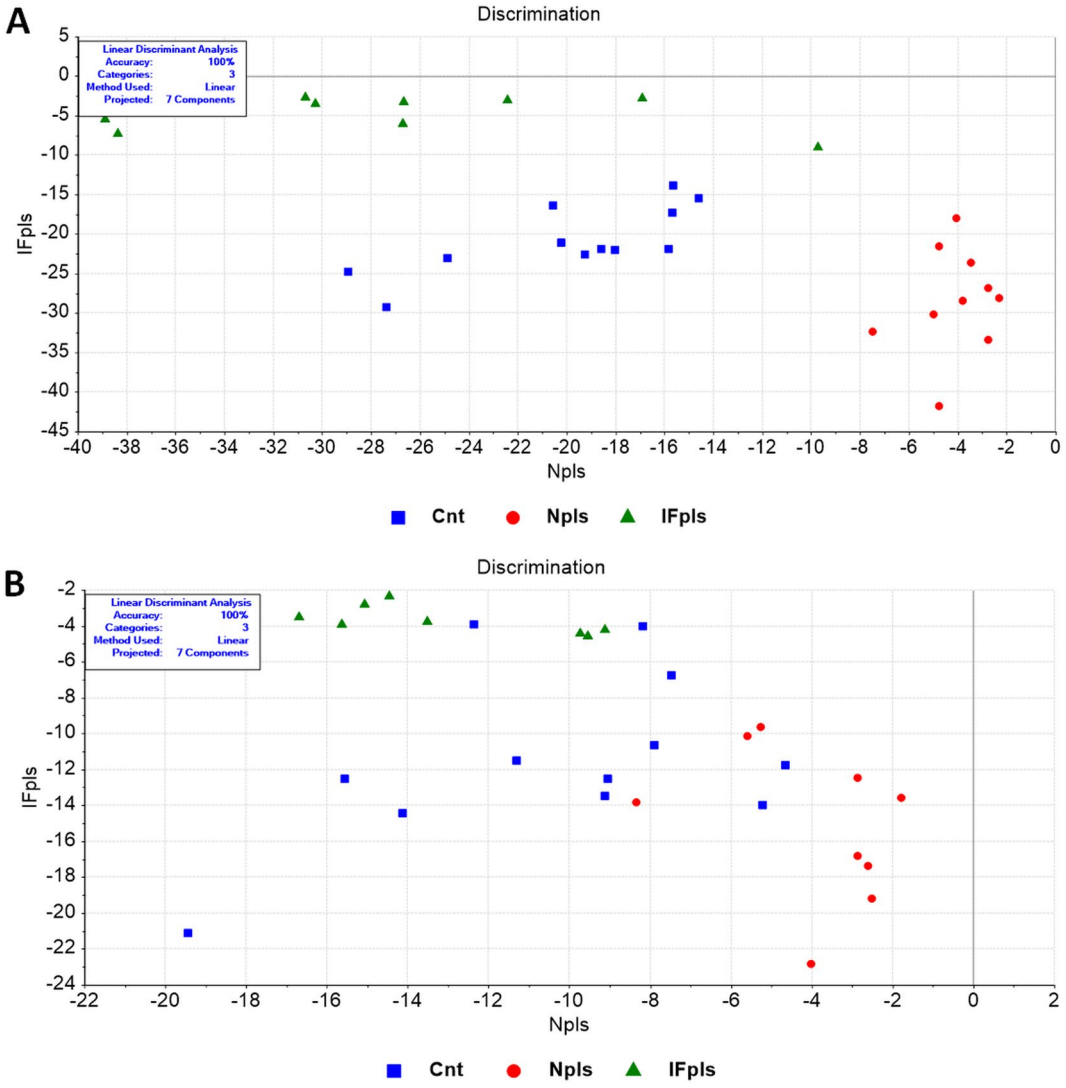

Fig. 1. LDA discrimination plot for tissue samples in full (4000–650 cm^{-1}) spectral region; **(A)** ileum and **(B)** colon. Cnt (control) group, IFpls (the group receiving plasma from rats undergoing intermittent fasting), and Npls (the group receiving plasma from untreated rats).

epithelium and muscular layer were intact, and the ileum's intestinal villi were abundant and systematically arranged, as shown in Fig. 5A. Furthermore, in the group that received plasma from IFpls rats, there was a more noticeable improvement in the histological structure of the ileum and colon compared to the group that received Npls plasma. The mucosal structure appeared more regular, and the epithelial cells were more prominent.

Histological examination revealed changes in the densities of goblet and Paneth cells between the control and treatment groups. In the ileum and colon sections of the control group, goblet cell densities were decreased, while a noticeable increase was observed in the IFpls recipient group. A decrease in Paneth cell densities was observed in the ileum samples of the control group, yet there was a significant increase in the IFpls recipient group (Fig. 4B). These findings highlight the positive impact of IFpls administration on aged gut health and structure, unveiling potential areas of damage and mitigation in aging. Also, aged mice's colon samples showed an increase in mucosal necrotic areas and glandular hyperplasia, along with a decrease in goblet cell density due to increased lymphatic infiltration (Fig. 5B). Conversely, these pathologies were resolved in the groups receiving Npls and IFpls. However, the remedial effects of IFpls were more effective than those of Npls (Fig. 5B).

In terms of the small intestine's physiology, cell divisions on the crypt floors are a regular biological process. Examining gerontological variations in crypt cell cycle duration, in terms of cell proliferation density, the ileum crypts' mitotic figures were more prominent in aged rats than in those given Npls and IFpls (Figs. 4 and 5).

IF-plasma reduces age-associated intestinal inflammation

The one of the target of our investigation was on the assessment of the inflammatory state in the aged ileum and colon tissues because inflammation is a hallmark of the aged rats. H&E-stained sections from the ileum and colon of aged rats exhibited enhanced lymphatic infiltration, indicative of inflammatory cells. Notably, the

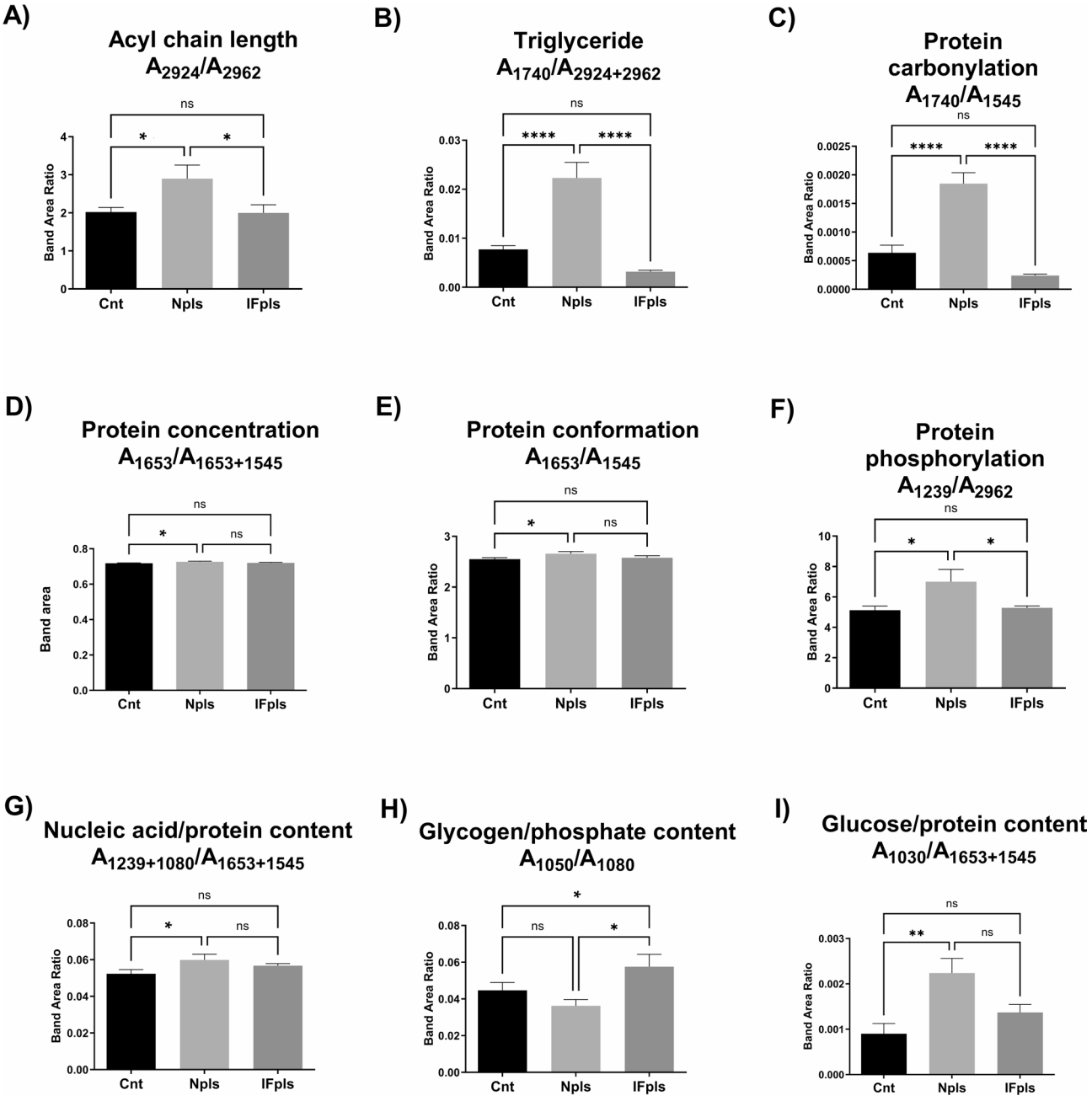

Fig. 2. The quantitative changes in lipid, polysaccharide, and nucleic acid-associated spectrochemical parameters for ileum sampels. The indices for band area ratio; **(A)** Acyl chain length of fatty acids (A_{2922}/A_{2955}), **(B)** Triglyceride content ($A_{1740}/_{A2924+2962}$), **(C)** Protein carbonylation (A_{1740}/A_{1545}), **(D)** Protein concentration ($A_{1653}/A_{1653+1545}$), **(E)** Protein conformation (A_{1653}/A_{1545}), **(F)** Protein phosphorylation ($A_{1239/}A_{2962}$), **(G)** Nucleic acid/protein content ($A_{1239+1080}/A_{1653+1545}$), **(H)** Glycogen/phosphate content (A_{1050}/A_{1080}) and **(I)** Glucose/protein ($A_{1030}/A_{1653+1545}$). A (Absorbance), Cnt (control) group, IFpls (the group receiving plasma from rats undergoing intermittent fasting), and Npls (the group receiving plasma from untreated rats).

severity of this lymphatic infiltration was significantly attenuated in the aged rats who received IFpls, when juxtaposed with the aged and Npls received group (Figs. 4A and 5A). The IFpls transfer to aged rats appeared to exert a strong positive influence on inhibition of inflammation encountered within the ileum and colon mucosa. These findings thus underscore the potential of Npls and IFpls transfer in mitigating the deleterious effects of aged ileum and colon on intestinal health.

Histomorphometric changes of ileum and colon tissues

Age-related changes have been linked to modifications in the height, length, thickness, and depth of ileum and colon tissues' histological structures. The compiled morphometric data for the ileum and colon are illustrated

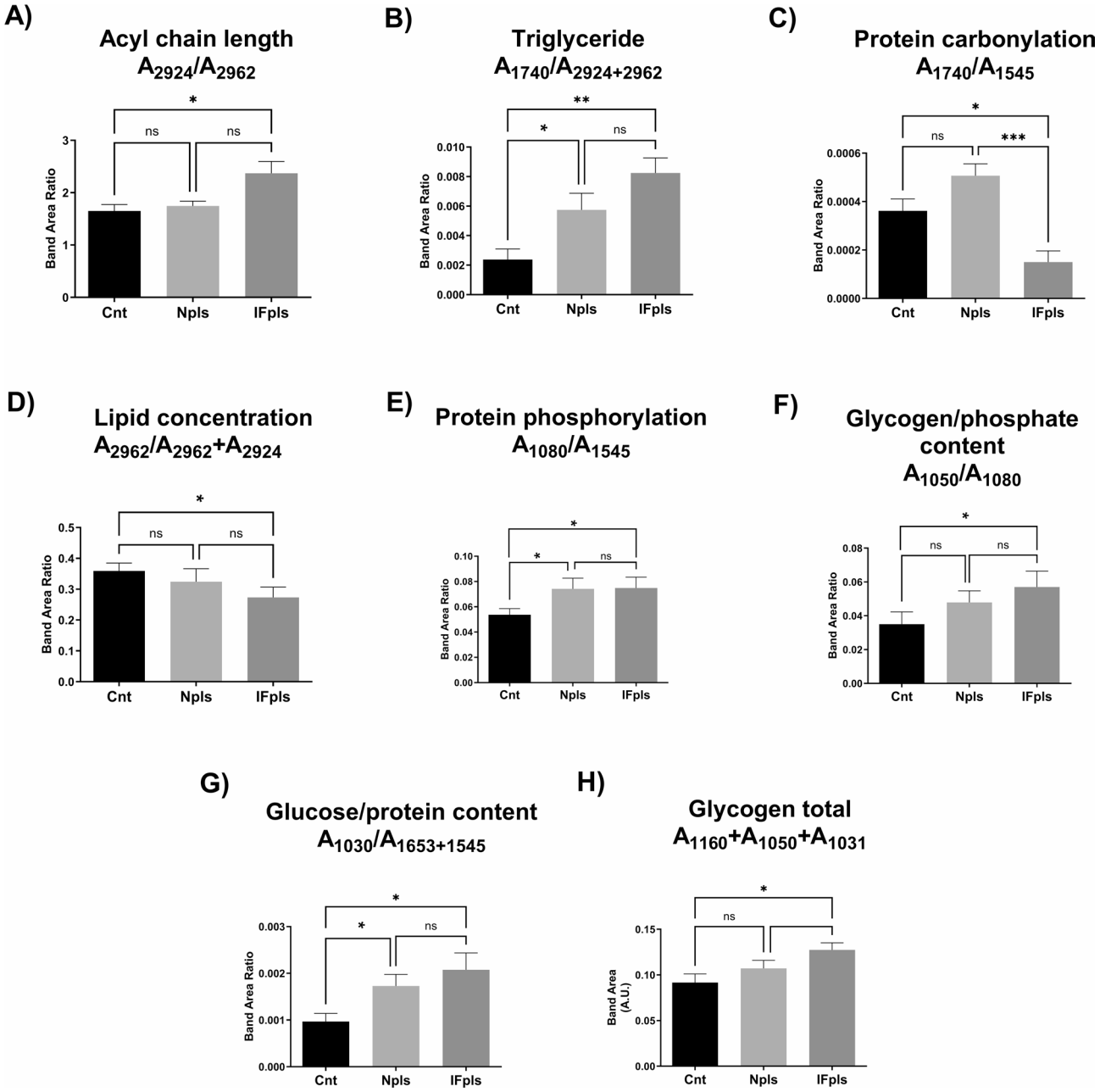

Fig. 3. The quantitative changes in lipid, polysaccharide, and nucleic acid-associated spectrochemical parameters for colon sampels. The indices for band area ratio; **(A)** Acyl chain length of fatty acids (A_{2924}/A_{2962}), **(B)** Triglyceride content ($A_{1740}/_{A2924+2962}$), **(C)** Protein carbonylation (A_{1740}/A_{1545}), **(D)** Lipid concentration ($A_{2962}/A_{2962+2924}$), **(E)** Protein phosphorylation (A_{180}/A_{1045}), **(F)** Glycogen/phosphate content (A_{1050}/A_{1080}), **(G)** Glucose/protein ($A_{1030}/A_{1653+1545}$), **(H)** Glycogen total ($A_{1160} + A_{1050} + A_{1031}$). A (Absorbance), Cnt (control) group, IFpls (the group receiving plasma from rats undergoing intermittent fasting), and Npls (the group receiving plasma from untreated rats).

in Figures S7 and S8, respectively. Significant variations in the lengths of the ileum and colon were observed in both Npls and IFpls recipient groups. We scrutinized histomorphometric data from ileum and colon tissues for intestinal measurements, including the height of the villi, the depth of the crypts, the thickness of the mucosa and submucosa, and the overall thickness of the intestinal wall.

Our findings showed that in aged rats, there were reductions in villus lengths, crypt depths, and mucosa and muscle layer thickness, while submucosal and total wall lengths increased (Figure S7a, S7b, S7c, S7e, S7d, S7f). Interestingly, a significant increase in villus lengths, crypt depths, and mucosal and muscle layer thickness was observed in the aged group given IFpls, in comparison to the aged group (Figure S7a, S7b, S7c). In contrast, the ileum morphometric parameters in the Npls recipient group displayed similar trends to those in the IFpls recipient aged rats, yet no substantial difference was noted in the lengths of the submucosa and muscle layers

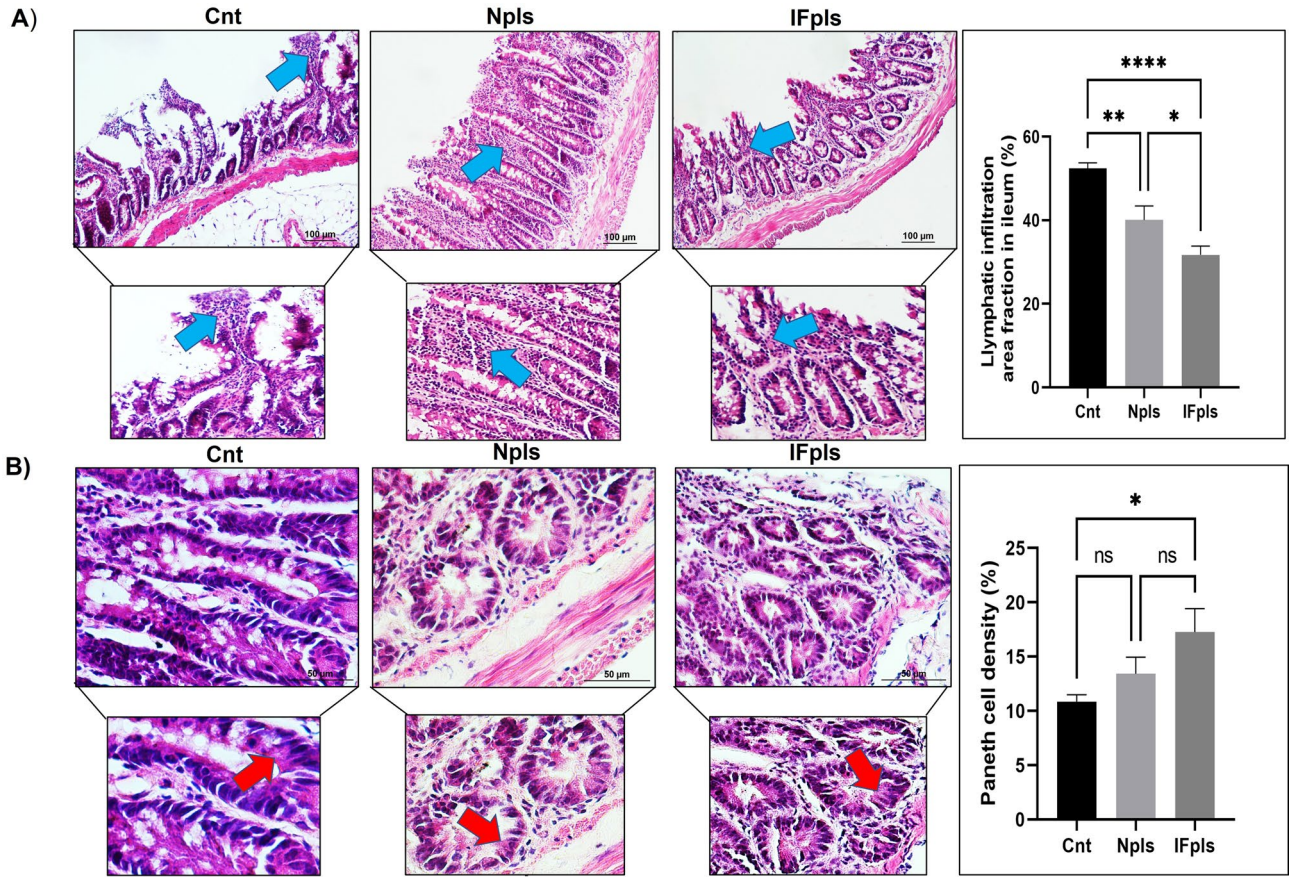

Fig. 4. Representative images of H&E staining and quantification of lymphatic infiltration area fraction (%) in all groups of ileum tissues (**A**). Aged rats ileum show increased lymphatic infiltration, but IF plasma received aged groups improved these histopathological alterations. Blue arrow shows lymphatic infiltrates. Representative images of H&E staining and quantification of Paneth cells intensity of area fraction (%) in all groups of ileum tissues (**B**). Aged rats' ileum show decreased Paneth cells intensity, but IF plasma received aged groups display increased Paneth cell density (%). Red arrow shows Paneth cells. Areas in the H&E-stained microphotographs of all groups were magnified in the photos to which they belonged to the area of interest. Values are expressed as mean ± SEM; $n = 7$ rats in each group. The significance levels were stated as $p \leq 0.05$ *, $p \leq 0.01$ **, and $p \leq 0.0001$ **** (nonparametric Mann-Whitney U test). Scale bar = 50 µm and 100 µm. Cnt (control) group, IFpls (the group receiving plasma from rats undergoing intermittent fasting), and Npls (the group receiving plasma from untreated rats).

of both groups (Figure S7d, S7e). According to these results, IFpls administration significantly improved every assessed histomorphometric parameter in the ileum of aged rats.

A comprehensive analysis of the morphometric parameters of colon tissues from all groups is presented in Figure S8. We evaluated the crypt depth, mucosa, submucosa, muscle layer, and total wall thickness of the colon tissues. Our findings revealed an increase in submucosa, muscle layer, and total wall lengths, coupled with a decrease in crypt depths and mucosal lengths in the aged rat group. In contrast, in the aged group given IFpls (Figure S8c, S8d, S8e), there was a significant decrease in submucosa, muscle layer, and total wall lengths, alongside a noticeable increase in crypt depths and mucosal lengths. Although the effects of Npls were not as pronounced as IFpls, morphometric changes similar to those observed in the IFpls recipient group were noticed in the colons of aged rats given Npls.

Quantitative analysis of rat serosal mast cells density in the ileum and colon

Considering the association of mast cells with age-related intestinal damage, we aimed to elucidate their role in our study. By staining slices of the ileum and colon with toluidine blue (TB), a dye that induces metachromasia in mast cells, we could examine the densities of these violet-purple mast cells in the ileum and colon sections. The aged group displayed a prevalent mast cell density in the intestinal serosa layers of ileum and colon sections. In stark contrast, a significant decrease in mast cell density was observed in the Npls and IFpls recipient aged rats compared to the aged group. In both the Npls and IFpls groups, the intestinal mast cells were easily distinguishable, with their contained granules generally appearing homogeneous. The serosal mast cell density (in both the ileum and colon) was significantly higher in the aged group compared to the Npls and IFpls recipient groups (Fig. S9 and Fig. S10). Additionally, areas with increased mast cell density in the aged group also exhibited a greater

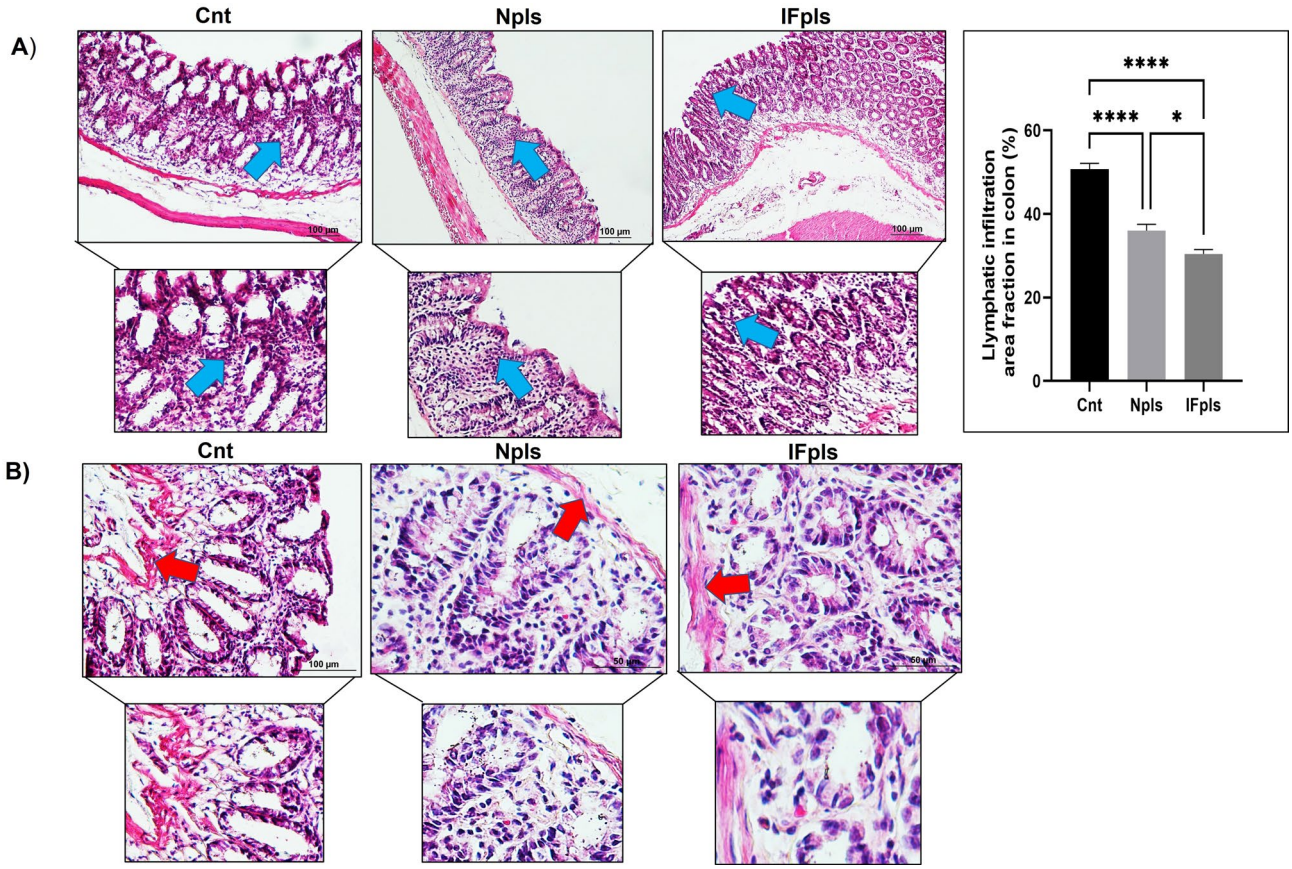

Fig. 5. Representative images of H&E staining and quantification of lymphatic infiltration area fraction (%) in all groups of colon sections (**A**). Aged rats colon show increased lymphatic infiltration, but IF plasma received aged groups improved these histopathological alterations. Representative images of H&E staining and degenerations of muscularis mucosa in all groups of colon sections (**B**). Remarkable necrotic degenerations were seen in the muscularis mucosal areas of the colon of aged mice, but IF plasma ameliorated these histopathological changes in the aged group. Red arrow shows muscularis mucosa. Areas in the H&E-stained microphotographs of all groups were magnified in the photos to which they belonged to the area of interest. Values are expressed as mean ± SEM; $n = 7$ rats in each group. $p \leq 0.01$ **, and $p \leq 0.0001$ **** (nonparametric Mann-Whitney U test). Scale bar = 100 µm. Cnt (control) group, IFpls (the group receiving plasma from rats undergoing intermittent fasting), and Npls (the group receiving plasma from untreated rats).

concentration of granules (Fig. S9 and Fig. S10). Therefore, we revealed a significant correlation between mast cell count and intestinal inflammation in aged rats. These findings underscore the potential of IFpls in reducing mast cell proliferation, thereby potentially alleviating intestinal inflammation.

IF plasma reduces intestinal inflammation and alters inflammatory factors of TNF-α and COX-2 expressions in the aged ileum and colon

We assessed the effects of Npls and IFpls transfers on the production of inflammatory enzymes TNF-α and COX-2, typically elevated in the ileum and colon tissues of aged rats. Immunochemical analyses of TNF-α and COX-2 expressions in the ileum and colon of control and treatment groups are illustrated in Fig. 6A and B. Our findings showed that the expressions of TNF-α and COX-2 in the ileum and colon of aged rats administered with IFpls were less intense compared to the other groups. The expressions of TNF-α in the aged rat's ileum and colon significantly increased compared with the Npls recipient group. TNF-α positive stained cells predominantly located within mucosa (lamina propria) and submucosa, displayed brown-yellow cytoplasm. Administration of IFpls resulted in a significant reduction of TNF-α expressions in ileum and colon tissues. Expressions of TNF-α significantly weakened in an age-dependent manner in the group not given plasma compared with the aged rat group ($p \leq 0.0001$ ****, see Fig. 6A and B). The inhibitory effects of IFpls on COX-2 expression were noticeable by a significant decrease in IFpls-treated aged rats in both ileum and colon tissues. Further, Fig. 6A and B show the intensity of COX-2 immunostaining appears increased in the aged rats group compared to the other groups. In the Npls recipient group, COX-2 expression was scarcely found in the mucosa and submucosa. Compared with other groups, the expression of COX-2 was observed to be elevated in cells of the surface epithelium and in cells of the inflammatory infiltrate in the aged rats group.

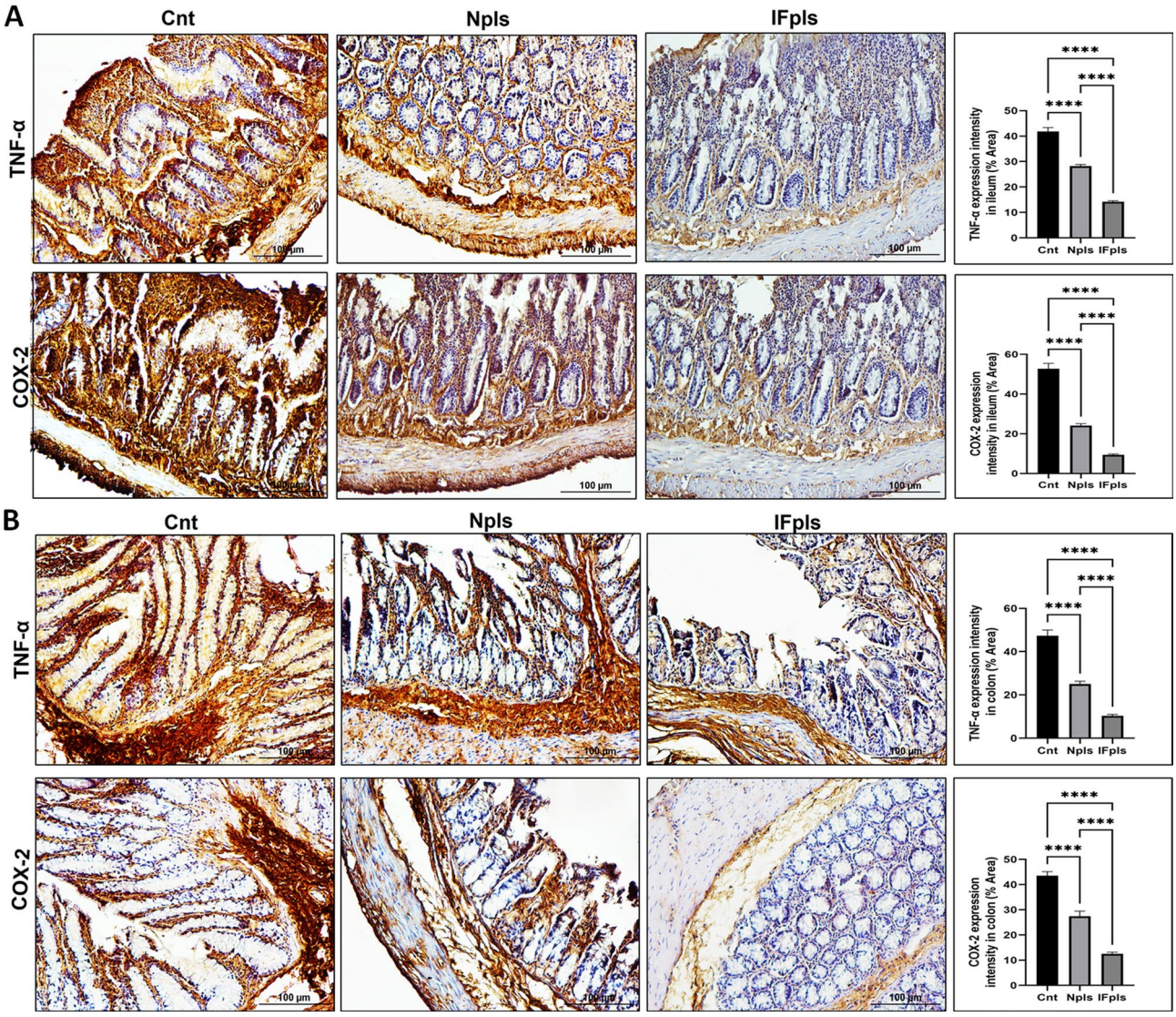

Fig. 6. Assessment of TNF-α and COX-2 expression in rat ileum (**A**) and colon (**B**); presents the Immuno Histo Chemistry (IHC) staining images displaying the expression levels of TNF-α (Tumor Necrosis Factor-alpha) and COX-2 (Cyclooxygenase-2). The bar graphs represent the staining intensity of TNF-α and COX-2, quantified using ImageJ (FIJI) software. The changes in staining intensity provide insights into the alterations in these inflammatory markers. Cnt (control) group, IFpls (the group receiving plasma from rats undergoing intermittent fasting), and Npls (the group receiving plasma from untreated rats).

Gut microbiota analysis

Alfa diversity and F/B ratio changed differently

In this study, metagenomic analysis was used to compare alpha diversity indexes between groups by analyzing the amplicon sequences. The Anova results showed a significant difference in Shannon value between the groups. When compared to the control group, there was a significant increase in species diversity in the group IFpls where plasma from rats with intermittent fasting was transferred, while there was no significant change in the group where normal blood plasma from rats without any treatment was transferred (Npls). The Shannon value was significantly different between the IFpls and Npls groups (Fig. 7A). A similar situation was observed in terms of Simpson's value, which expresses the prevalence of species found in GM. The Anova result between the groups was significant. In the comparison of the groups with each other, the Simpson value increased significantly in the IFpls group when compared with control, while there was no change in the Npls group. The Simpson value was also found to be significantly higher in the IFpls group compared to the Npls group (Fig. 7B). There was also a significant difference between the groups in terms of Firmicutes to Bacteroidetes ratios (F/B). When the groups were compared with each other, there was a significant difference only between the IFpls and Npls groups (Fig. 7C).

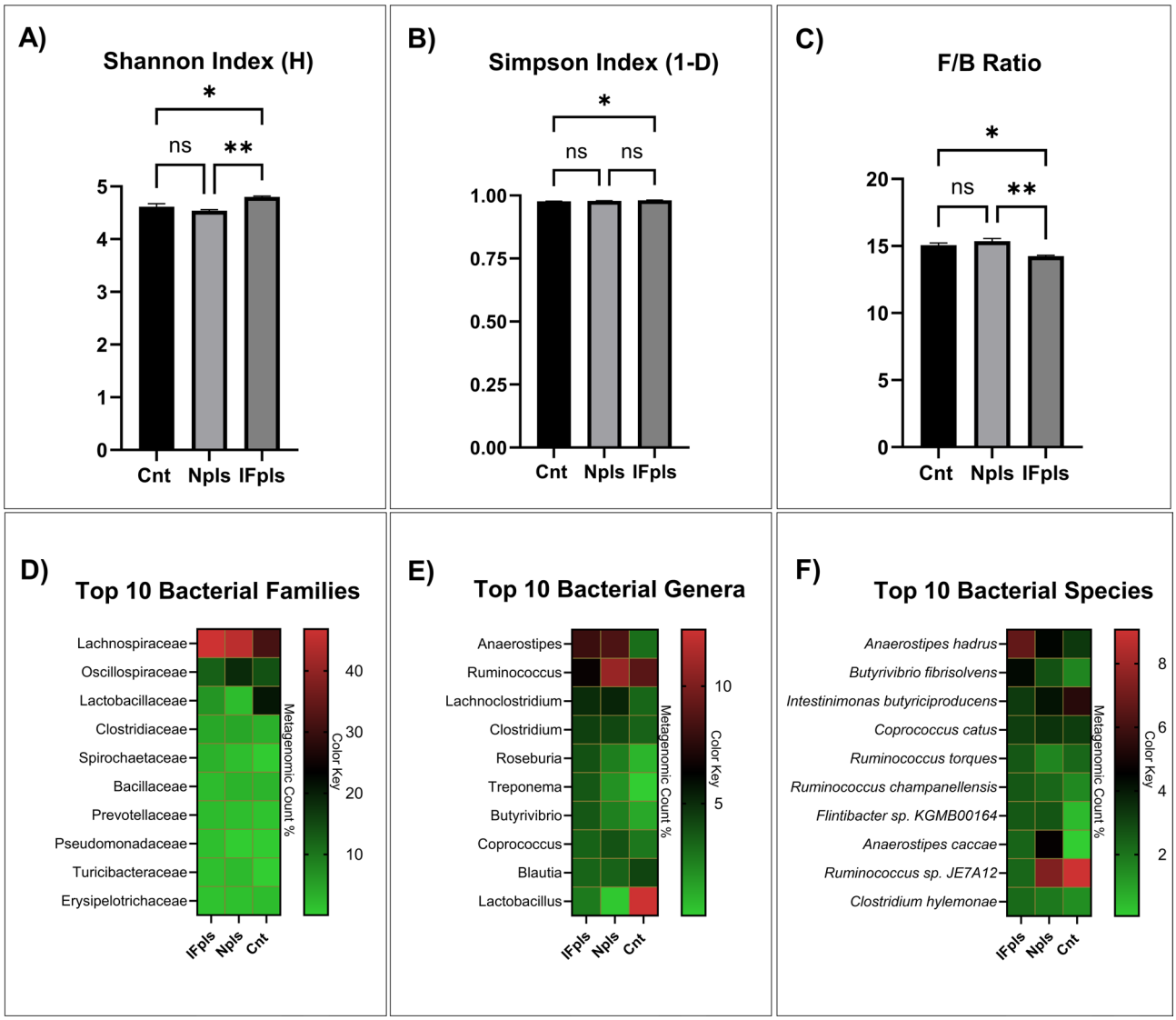

Fig. 7. The effects of plasma from rats with intermittent fasting and plasma from rats without any treatment on the rats' gut mikrobiota **(A)** Shannon (H), **(B)** Simpson (1-D) indexes and **(C)** Firmicutes to Bacteroidetes ratio (F/B ratio). One-way anova (one-sided p-value) was utilized. The degree of significance was denoted as * $p < 0.05$, ** $p < 0.01$, *** $p < 0.001$, and **** $p < 0.0001$. Heatmaps showing a comparison of the percent metagenomic ratios of the top ten bacterial **(D)** families, **(E)** genera and **(F)** species that became dominant after IFpls transfer in the Cnt and Npls groups. Cnt (control) group, IFpls (the group receiving plasma from rats undergoing intermittent fasting), and Npls (the group receiving plasma from untreated rats).

The top ten bacterial families, genera and species have been reshaped

Differences occurred in the dominant bacterial families after the plasma treatments (Table S17). More changes occurred in the IFpls group compared to the Cnt group. The bacterial families Spirochaetaceae, Pseudomonadaceae, and Turicibacteraceae were found among the dominant top ten only in the IFpls group. The bacterial families Turicibacteraceae and Spirochaetaceae were included only in the Npls group. This difference between the groups also occurred in terms of the top ten genera most dominantly. A comparison of the first ten bacterial families predominantly found in the IFpls group with the prevalence in other groups is shown in Fig. 7D. Similarly, more changes occurred in the IFpls group genus compared to Cnt (Table S18). The genus Roseburia, Treponema and Butyrivibrio became dominant only in the IFpls group, while the ordering of common genera varied with different incidence rates. The Npl group had a more similar profile to Cnt. Mediterraneibacter and Anaerocolumna were among the top ten dominant genera only in the Npls group. The Liglactobacillus genus was suppressed in both the IFpls and Npls groups. A comparison of the first ten bacterial genera predominantly found in the IFpls group with the prevalence in other groups is shown in Fig. 7E.

Plasma applications also show the greatest effect at the species level (Table S19). *Anaerostipes hadrus*, *Ruminococcus sp.* JE7A12, *Intestinimonas butyriciproducens* and *Coprococcus catus* species were among the top ten dominant species in all three groups. More common species were found between IFpls and Npls. *Butyrivibrio*

fibrisolvens, *Flintibacter sp.* KGMB00164, and *Ruminococcus champanellensis* were only included in the IFpls and Npls groups. *Clostridium hylemonae* was only in the IFpls group, while *Flavonifractor plautii* could only become dominant in the Npls group. *Bacillus velezensis* was dominant in the Cnt and Npls groups with different incidence rates. In addition, a comparison of the first ten bacterial species predominantly found in the IFpls group with the prevalence in other groups is shown in Fig. 7F.

Short chain fatty acid (SCFA) analysis

The study rigorously quantified the concentrations of short-chain fatty acids (SCFAs) within the cecal contents. The data revealed statistically significant discrepancies across various experimental cohorts. Upon administration of fasting-induced plasma (IFpls) and normal plasma (Npls), a pronounced increase in acetic acid levels was observed, with the most significant elevation detected in the IFpls cohort, as depicted in Supplementary Figure S11a. This suggests that the fasting-induced plasma modulates the production or accumulation of acetic acid more effectively than normal plasma. Regarding butyric acid, the IFpls group exhibited a noteworthy increment when compared to the Npls group, underscoring the potential influence of fasting plasma on butyric acid concentration. However, this increase did not reach statistical significance when the IFpls group was compared to the untreated control group, as shown in Supplementary Figure S11b. This indicates a nuanced effect of fasting plasma on butyric acid levels that requires further investigation. The isovaleric acid concentration was found to be significantly elevated in the IFpls group relative to the control, suggesting a specific response to fasting-induced plasma, as illustrated in Supplementary Figure S11c. Conversely, the Npls group did not show such a differential, indicating a unique influence of the fasting state on this SCFA. Finally, isobutyric acid levels were significantly higher in the IFpls group when compared to both the control and Npls groups, as presented in Supplementary Figure S11d. This finding points to a potential fasting-specific biochemical pathway or microbial interaction leading to increased isobutyric acid production. These findings imply that fasting-induced plasma plays a unique role in altering the cecal SCFA profile, which may have significant implications for gut health and warrants further exploration into the underlying mechanisms governing these changes.

Discussion

The results of this study elucidate the profound impact that intermittent fasting plasma transfer exerts on the biomolecular architecture and structural integrity of intestinal tissues in elderly rodents. The ensuing discussion seeks to critically examine these findings within the existing literature on gerontological health and gastrointestinal physiology. By delving into the nuanced interactions between IF-induced plasma alterations and cellular mechanisms, this analysis aims to enhance our understanding of the tissue-specific responses observed. Moreover, the reduction in inflammatory markers and the modulation of gut microbiota composition observed in our experiments provide a compelling argument for the potential of IF as a therapeutic intervention to ameliorate age-related degenerative changes in the gut. Through this discourse, we aim to delineate the underlying biochemical pathways that are influenced by IF, potentially paving the way for novel approaches to foster healthy aging.

The histological and histomorphometric analyses showed that, the pronounced impacts of IFpls on the structural integrity and health of the gut became strikingly evident. In tandem with these changes, our research shone a light on IFpls' ability to drive a significant attenuation of age-related inflammation, manifested in reduced lymphatic infiltration in the gut tissues, which suggests a potential anti-inflammatory role of intermittent fasting. Our study aligns with existing literature, shedding light on the inflammation and protein modification that escalate with age, fostering an environment conducive for reactive oxygen species generation and subsequent protein modification[24–27]. This domino effect results in lymphatic infiltration, coupled with increased protein carbonylation, a well-documented phenomenon in aging. We found that the significantly higher lymphatic infiltration observed in aged rats was markedly reduced following IFpls treatment. The significant decrease in protein carbonylation value in both ileum and colon tissues after IFpls in IR spectrochemical band analyzes also supports these results. However, it was noted that this value increased in both tissues after Npls.

Aging is associated with increased lipid peroxidation, leading to oxidative damage[28]. Such damage is exhibited as morpho-quantitative alterations in the histology of the ileum and colon, which may compromise intestinal function. Intriguingly, our data indicates that the administration of both treatment especially IFpls can reverse these aging-induced morphological changes in rats, demonstrating a protective and restorative effect on ileum and colon histology. Previous research emphasizes that age-related decline and loss of epithelial cells in the ileum and colon lead to decreased goblet cell density, thereby disrupting the epithelial intestinal barrier[29–31]. Our findings, exhibiting a reduction in intestinal goblet cell densities in aged rats, align with this evidence. Notably, the administration of both treatments, particularly the IFpls, resulted in an increase in goblet cell density in the ileum and colon. This suggests their potential to counteract the age-induced decline in epithelial barrier integrity through positive modulation of goblet cell functionality. In addition, our study observed the emergence of mitotic figures in the mucosal areas of aged ileum and colon samples, indicating the activation of crypt stem cells in response to age-induced cellular damage. Complementing this, we found that the regenerative effects of both Npls and IFpls, particularly IFpls, on epithelial cells are reinforced by modifications in the biomolecular composition of ileum and colon tissues. Collectively, these findings underscore the potential of IFpls and, to a lesser extent, Npls as promising therapeutic strategies for mitigating aging-related changes.

Mast cells are integral components of the immune system, and their roles in aging-related chronic diseases have been increasingly recognized[32]. Aging notably influences mast cell physiology, their involvement in immunological events, and their inflammatory or other biological responses[33]. Past research has identified an increase in local or systemic mast cell densities in various pathological conditions, including metabolic and neoplastic diseases, as well as aging[34–36]. In this context, a rise in mast cell populations is linked with chronic disease progression[37]. Therefore, cellular damage ensuing from mast cell degranulation may significantly affect

the severity of prevalent diseases in aging biology. Given this understanding, we explored alterations in mast cell populations in the ileum and colon, as well as the expression levels of inflammatory mediators such as TNF-α and COX-2 cytokines, to elucidate the impact of both Npls and IFpls transfers on intestinal cellular damage and inflammation that occur with aging. Our findings demonstrated a significant increase in the degranulation and density of serosal mast cells due to inflammation in the ileum and colon samples of the control group. However, Npls and IFpls administration remarkably attenuated these increases in mast cells. It is apparent that with the rise in mast cell densities in aged rats, there is an escalation in oxidative stress and inflammation in the ileum and colon. Our immunohistochemistry results affirm this association. Notably, we observed a significant decrease in the expression intensities of TNF-α and COX-2 after both treatments particularly with the IFpls.

The enhancements in gut microbiota diversity following IF plasma transfusion observed in this study provide critical insights into the complex relationship between dietary interventions, microbial diversity, and aging. Our findings reveal that plasma from IF-treated rats significantly boosts microbial alpha diversity in aged counterparts, suggesting a potential avenue for moderating age-related microbial imbalances[38]. This aligns with prior research indicating that both young plasma and IF regimes enhance gut microbiota diversity, offering a strategic approach to foster a healthier gut ecosystem in elderly populations[19]. Despite notable improvements, the Firmicutes/Bacteroidetes (F/B) ratio a crucial indicator of gut health did not fully normalize, underscoring the persistence of age-related dysbiosis. This partial modulation of the F/B ratio is consistent with findings by Indiani et al. (2018), who documented shifts in this ratio across life stages[39]. Furthermore, a study by Li et al. (2017) on the core microbiota of Sprague-Dawley rats[40], the model organism used in our study, identified a predominance of Firmicutes, mirroring our control group's dysbiotic structure. The significant yet incomplete reduction in the F/B ratio observed post-transfusion underscores the nuanced role of Firmicutes and Bacteroidetes in producing SCFAs, crucial for intestinal epithelial health and highlighted in[41] as pivotal in aging gut microbiota dynamics. This multifaceted interaction between diet, microbial ecology, and aging invites further exploration to fully harness dietary strategies for improving elderly gut health and overall well-being.

The increased levels of acetic, butyric, isovaleric, and isobutyric acids in the cecum of aged rats treated with IF plasma (IFpls) compared to non-fasting plasma (Npls) and controls highlight IFpls' potential to promote a healthier gut microbiome. Notably, the surge in acetic acid suggests a shift toward a microflora that enhances fermentative activities and potentially improves gut barrier functions and inflammatory responses. While butyric acid levels were not markedly higher than controls, their increase under IFpls indicates a positive, albeit partial, effect on colonic health. The notable increases in isovaleric and isobutyric acids in the IFpls group may reflect a unique metabolic pattern induced by intermittent fasting, possibly due to the selective growth of bacteria that metabolize branched-chain amino acids. These findings suggest that diet-induced changes in plasma can significantly influence gut microbial metabolism, offering new insights into managing age-related declines in gut health through dietary strategies that modulate the gut microbiota.

In summary, this study highlights that IF plasma transfer significantly affects the biomolecular and structural aspects of intestinal tissues in aged rats, promoting gut health. The plasma from fasting rats modifies lipid, protein, and nucleic acid profiles in a tissue-specific manner, reduces inflammation, and improves gut structure. Key findings include decreased mast cell density and lower levels of inflammatory cytokines such as TNF-α and COX-2, particularly in the IF-treated groups. Metagenomic sequencing showed enhanced microbial diversity and a favorable Firmicutes to Bacteroidetes ratio. Importantly, an increase in beneficial SCFAs was noted, suggesting enhanced metabolic functions of gut microbiota. These findings suggest that IF plasma transfer could be a novel method to mitigate aging effects on the gut, offering a promising therapeutic strategy for healthy aging.

Methods

Animal studies

Intermittent fasting regime was applied to the Sprague Dawley rats (12-month-old, $n = 17$) for 35 days. Rats in the intermittent fasting (IF) group had unrestricted access to water; however, their food intake was limited to a 6-hour feeding window following an 18-hour fasting period. The designated feeding period was between 09:00 a.m. and 03:00 p.m. Following 35 days of intermittent fasting, plasma samples were collected from both the IF group ($n = 17$) and age-matched control rats that had not undergone any treatment ($n = 17$)[19,42]. Subsequently, plasma from the IF-treated rats was administered to a separate group of 24-month-old Sprague Dawley rats ($n = 7$), while plasma from untreated control rats was administered to another group of aged Sprague Dawley rats ($n = 7$). Plasma was delivered intraperitoneally at a volume of 0.5 mL per rat, every other day, for a total of 15 administrations. A third group of aged rats ($n = 7$) served as controls and did not receive any plasma treatment. The volume of blood plasma transferred was determined as 1/10th of the animal's total blood plasma volume. Rats in each group were housed in separate Plexiglas cages (7 rats per cage) to avoid cross-contamination, with all co-housed rats remaining within the same experimental group throughout the study[9,19,38].

This study was approved by the Saki Yenilli Experimental Animal Production and Practice Laboratory Ethics Committee (meeting date: 05/03/2021, approval number: 2021/05). All experimental protocols were carried out in accordance with institutional guidelines. Additionally, this study adheres to the ARRIVE (Animal Research: Reporting of In Vivo Experiments) guidelines (https://arriveguidelines.org). All animals were housed under standard laboratory conditions with ad libitum access to food and water, maintained on a 12-hour light/dark cycle at a constant temperature of 21 °C. At the conclusion of the experimental period, animals were humanely euthanized in accordance with the AVMA Guidelines for the Euthanasia of Animals (2020). Euthanasia was performed using a carbon dioxide (CO_2) chamber, with CO_2 introduced at a flow rate sufficient to displace 30–70% of the chamber volume per minute. Following loss of consciousness, exposure to CO_2 was continued for several minutes to ensure death.

For metagenomic analysis, intestinal tissue samples, including the cecal region and its contents, were collected and immediately flash-frozen using dry ice, then stored at − 80 °C until further processing. For spectrochemical

analysis, tissues from the ileum and colon were similarly harvested, flash-frozen on dry ice, and preserved at − 80 °C until analysis. For histopathological examination, additional ileum and colon tissue samples were collected and fixed in 10% neutral-buffered formalin until further evaluation[20].

Plasma collection

Animals were rendered unconscious using CO_2 in accordance with the AVMA Guidelines for the Euthanasia of Animals (2020), as described previously. Plasma samples were obtained via intracardiac puncture at the time of euthanasia. Blood was collected into EDTA-containing tubes and centrifuged at 1,000 × g to separate the plasma. To denature proteins, the plasma was heated at 95 °C for 2–3 min, followed by centrifugation at 1,000 × g for 15 min at 4 °C. All plasma aliquots were stored at − 80 °C until use. Prior to administration, EDTA was removed from the plasma using 3.5-kDa D-tube dialyzers (EMD Millipore) against phosphate-buffered saline (PBS)[9,38].

Gut microbiota analysis

DNA isolation

Genomic DNA isolated from cecum content by Quick DNA TM Fecal/Soil Microbe Miniprep Kit (Cat. No: D6010). The amount and purity of the isolated DNA were determined fluorometrically by Qubit fluorometer[19,38].

Amplification of the 16 s rRNA V3-V4 region

V3-V4 regions of the 16 s rRNA gene to be used for species determination were amplified with universal 341 F (CCTACGGGNGGCWGCAG) and 805R (GACTACHVGGGTATCTAATCC) primer sequences using SimpliAmp Thermal Cycler[19,38].

PCR conditions of 16 s V3–V4 regions

PCR conditions: 95 °C 10 min, first denaturation (HS enzyme will be used), 35 cycles: 95 °C for 45 s – denaturation, 50–55 °C for 45 s – adhesion, 72 °C for 60 s, elongation, 72 °C for 3 min – final elongation, the temperature was reduced to 4 °C and PCR was completed[19,38].

Library Preparation and sequencing

Illumina's Nextera XT DNA Library Prep Kit (Cat. No: FC-131-1096) was used to prepare the library for the 16 s rRNA V3-V4 amplicon products, and the TG Nextera XT Index Kit v2 Set A (Cat. No: TG-131-2001) was used to index the library. Beckman Coulter's AMPure XP beads were used for PCR purification. Illumina's Miseq technology was utilized to sequence the data as paired end (PE) 2 × 150 base reads. Each sample had a minimum of 30,000 readings[19,38,43]. Metagenome sequencing was performed at Ficus Biotechnology (FicusBio), Ankara, Turkey.

Bioinformatics analysis of Raw data

The raw sequence data (FastQ) was subjected to quality checks to increase the accuracy of microbial diversity estimation and to filter out sequencing artifacts such as low-quality and contaminated reads, followed by trimming using FastQC v0.10.1 when required. The Kraken Metagenomic system was used to cluster the sequence data into OTU groups[44]. Heatmaps were created with GraphPad Prism 10.03 (GraphPad Software, USA) software.

Alfa diversity indexes

Alpha diversity indices were calculated at the species level. Shannon's Equitability Index values typically range between 1.5 and 3.5, with higher values indicating a more even distribution of species. Simpson's Diversity Index (1–D) was calculated based on both the abundance and evenness of operational taxonomic units (OTUs), yielding a value between 0 and 1, where values closer to 1 indicate greater diversity and evenness within the community[19,38].

Short chain fatty acid (SCFA) analysis

To determine short-chain fatty acid (SCFA) levels, 1 g of cecal content from both control and experimental groups was collected and transferred into 2 mL Eppendorf tubes, followed by the addition of 1 mL of distilled water. The samples were centrifuged at 14,000 rpm for 5 min, and the resulting supernatants were collected. These supernatants were then filtered through 0.22 µm cellulose-acetate filters (Isolab). For High-Performance Liquid Chromatography (HPLC) analysis, the filtered samples were diluted threefold with ultrapure water[45].

SCFA analysis was conducted using a Shimadzu 20 A series HPLC system equipped with a UV detector (Shimadzu FCV-10AT). Separation was achieved using a Transgenomic ICSep ICE-COREGEL 87H3 ion-exchange column (300 mm × 7.8 mm). The mobile phase consisted of 0.088 M sulfuric acid, delivered at a flow rate of 0.6 mL/min. The column oven was maintained at 35 °C during analysis[45].

Infrared spectroscopy measurements

Ileum and colon samples of all animals were directly compressed on the Zn/Se crystal of the ATR unit (PerkinElmer) without any pretreatment and examined with an ATR-FTIR spectrometer (PerkinElmer) at a resolution of 4 cm^{-1} and a scan number of 32. The spectra were obtained with the Spectrum One (PerkinElmer) software in the wavelength range of 4000–650 cm-1[46].

Infrared spectral data analyses

Linear Discriminant Analysis (LDA) technique was applied to differentiate experimental groups. Sample spectra were preprocessed and subjected to Principal Component Analysis (PCA) using The Unscrambler®

X 10.3 software. Spectra were examined in lipid (3000–2700 cm^{-1}), protein (1700–1500 cm^{-1}), nucleic acid (1200–650 cm^{-1}), and full (4000–650 cm^{-1}) with the Singular Value Decomposition (SVD) algorithm[42]. LDA, a supervised classifier, linearly transformed samples into a lower-dimensional space, using PCA data as inputs. The Unscrambler® X 10.3 software generated training sets from different sample categories, and results were presented as discrimination plots and confusion and prediction matrices[46].

Spectral band analysis was performed using OPUS 5.5 (Bruker) software. The average spectra of each sample were baseline corrected using the Rubberband correction method prior to the band quantification analyses. In detailed band analyses, the bands with the highest absorbance values in different spectral regions of the spectra were selected and the beginning and ending frequencies of the bands were determined with precision. The areas of bands specific to various biomolecules were analyzed by taking the integral areas of the determined frequency ranges with the OPUS 5.5 (Bruker) software. In addition, a virtual line was drawn vertically from the midpoint of the band baseline to the peak of the band, and the length of the line was measured with the help of a virtual ruler. Then, by marking the point where 0.75 times the length of the line coincides with the line, a horizontal line was drawn along the band from this point to calculate the bandwidth values[47].

Histopathological analysis

After tissue dissection, neutral-buffered formalin (10%) was used for the fixation of liver tissues for 48 h at room temperature followed by preparation of paraffin Sect. (5 µm thickness) using a rotary microtome (Leica Biosystems, Germany). The obtained sections were stained using hematoxylin & eosin stain (H&E) (Hematoxylin: Cas No: 517-28-2; Eosin: Cas No: 17372-87-1, Merck, Germany) for a general architecture of the liver tissue. H&E slides were used for evaluating general tissue characterization of the rat liver. To investigate histological changes, an average of 10–15 areas was evaluated by random sampling for each Sect[11]. Two researchers blindly conducted all microscopic analyses of the histopathological changes.

H&E staining

For H&E staining, the following steps were performed respectively. Initially, all slides in each group were deparaffinized with xylene, dehydrated with ethanol and placed in hematoxylin solution, then washed under running water. They were differentiated by acidic alcohol for a dip, and then immediately rinsed with water, after which the slides were placed in eosin for 3 min. The next steps were dehydration in ascending ethanol and clearing in xylene. Subsequently, the slides were mounted by entellan and visualized using an Olympus BX53 microscope with an Olympus DP74 camera attachment[48].

Masson's trichrome (MT) staining

MT staining was performed according to the instructions provided in the kit 04-010802 (Bio-Optica, Milan, Italy) for detection of collagen accumulation of fibers in the rat liver. For MT staining, the tissue sections were deparaffinized and rehydrated, according to the kit. All procedures were carried out at room temperature[49].

Quantification of histopathological parameters

For histopathological evaluation of lymphatic infiltration and microvesicular steatosis (micro lipid droplets) in liver tissue stained with hematoxylin and eosin (H&E), grayscale binarization was performed using ImageJ Fiji (National Institutes of Health, Bethesda, MD, USA). A threshold was set at the lowest level sufficient to distinguish purple-stained (cellular) and non-stained regions, enabling quantification of area fractions (%) of interest. For Masson's Trichrome (MT) staining, grayscale binarization with a threshold optimized for detecting blue-stained regions was applied to quantify MT-positive areas. This quantification method was modified from Adomshick et al. (2020)[50]. For all animals within each group, signal intensities from five representative images per tissue section were quantified and presented graphically. All microphotographs of the sections were analyzed by the light microscopy (Olympus BX53, Japan) using a camera attachment (Olympus DP27, Japan) with imaging systems (Olympus cellSens Entry, Japan).

Statistics

The statistical analyses were given as mean ± standard error of the mean (SEM). An unpaired T test and One-way anova (one-sided p-value) was utilized to compare the alpha diversities and F/B ratio between IFpls and control Cnt and Npls groups. The comparison was done in GraphPad Prism 10.03 (GraphPad Software, USA) software. The degree of significance was denoted as * $p<0.05$, ** $p<0.01$, *** $p<0.001$, and **** $p<0.0001$. Heatmap analyses of metagenomic counts for bacterial families, genera, and species between groups were also performed in GraphPad Prism 10.03 (GraphPad Software, USA) software.

Data availability

All metagenomic raw reads from the samples have been deposited in the NCBI database under BioProject ID PRJNA890552. Any additional data generated or analyzed during this study are available from the corresponding author upon reasonable request.

Received: 7 October 2024; Accepted: 19 September 2025
Published online: 24 October 2025

References

1. Lynch, S. V. & Pedersen, O. The human intestinal Microbiome in health and disease. *N Engl. J. Med.* **375**, 2369–2379 (2016).
2. Qin, J. et al. A human gut microbial gene catalogue established by metagenomic sequencing. *Nature* **464**, 59–65 (2010).

3. Ceylani, T., Jakubowska-Doğru, E., Gurbanov, R., Teker, H. T. & Gozen, A. G. The effects of repeated antibiotic administration to juvenile BALB/c mice on the microbiota status and animal behavior at the adult age. *Heliyon* **4**, e00644 (2018).
4. Fukuda, S. et al. Bifidobacteria can protect from enteropathogenic infection through production of acetate. *Nature* **469**, 543–547 (2011).
5. Zhang, J. et al. A phylo-functional core of gut microbiota in healthy young Chinese cohorts across lifestyles, geography and ethnicities. *ISME J.* **9**, 1979–1990 (2015).
6. Badal, V. D. et al. The gut microbiome, aging, and longevity: A systematic review. *Nutrients* **12**, 1–25 (2020).
7. Kim, S. & Jazwinski, S. M. The gut microbiota and healthy aging: A Mini-Review. *Gerontology* **64**, 513–520 (2018).
8. Liu, A. et al. Young plasma reverses age-dependent alterations in hepatic function through the restoration of autophagy. *Aging Cell.* **17**, e12708 (2018).
9. Villeda, S. A. et al. Young blood reverses age-related impairments in cognitive function and synaptic plasticity in mice. *Nat. Med.* **20**, 659–663 (2014).
10. Taner, H. et al. Age – related differences in response to plasma exchange in male rat liver tissues: insights from histopathological and machine – learning assisted spectrochemical analyses. *Biogerontology* https://doi.org/10.1007/s10522-023-10032-3 (2023).
11. Erdogan, K., Ceylani, T., Teker, H. T., Sengil, A. Z. & Uysal, F. Young plasma transfer recovers decreased sperm counts and restores epigenetics in aged testis. *Exp. Gerontol.* **172**, 112042 (2023).
12. Baba, B. et al. Therapeutic potential of young plasma in reversing age-related liver inflammation via modulation of NLRP3 inflammasome and necroptosis. *Biogerontology* 26, (2025).
13. Villeda, S. A. et al. The ageing systemic milieu negatively regulates neurogenesis and cognitive function. *Nature* **477**, 90–94 (2011).
14. Ceylani, T., Allahverdi, H. & Teker, H. T. Role of age-related plasma in the diversity of gut bacteria. *Arch. Gerontol. Geriatr.* **111**, 105003 (2023).
15. Ceylani, T. et al. The rejuvenating influence of young plasma on aged intestine. *J. Cell. Mol. Med.* **27**, 2804–2816 (2023).
16. Longo, V. D. & Mattson, M. P. Fasting: molecular mechanisms and clinical applications. *Cell. Metab.* **19**, 181–192 (2014).
17. Shetty, A. K., Kodali, M., Upadhya, R. & Madhu, L. N. Emerging Anti-Aging Strategies - Scientific basis and efficacy. *Aging Dis.* **9**, 1165–1184 (2018).
18. de Cabo, R. & Mattson, M. P. Effects of intermittent fasting on Health, Aging, and disease. *N Engl. J. Med.* **381**, 2541–2551 (2019).
19. Teker, H. T. & Ceylani, T. Intermittent fasting supports the balance of the gut microbiota composition. *Int. Microbiol. Off J. Span. Soc. Microbiol.* **26**, 51–57 (2023).
20. Teker, H. T. et al. Supplementing probiotics during intermittent fasting proves more effective in restoring ileum and colon tissues in aged rats. *J. Cell. Mol. Med.* **28**, 1–13 (2024).
21. Ceylani, T., Teker, H. T., Samgane, G. & Gurbanov, R. Intermittent fasting-induced biomolecular modifications in rat tissues detected by ATR-FTIR spectroscopy and machine learning algorithms. *Anal. Biochem.* **654**, 114825 (2022).
22. Allahverdi, H. Exploring the therapeutic potential of plasma from intermittent fasting and untreated rats on aging-induced liver damage. *J. Cell. Mol. Med.* **28**, e18456 (2024).
23. Severcan, F. & Haris, P. I. *Vibrational Spectroscopy in Diagnosis and Screening*vol. 6 (IOS, 2012).
24. Wellman, A. S. et al. Intestinal epithelial Sirtuin 1 regulates intestinal inflammation during aging in mice by altering the intestinal microbiota. *Gastroenterology* **153**, 772–786 (2017).
25. Funk, M. C., Zhou, J. & Boutros, M. Ageing, metabolism and the intestine. *EMBO Rep.* **21**, 1–22 (2020).
26. Bana, B. & Cabreiro, F. The Microbiome and aging. *Annu. Rev. Genet.* **53**, 239–261 (2019).
27. Choudhary, P., Kathuria, D., Suri, S. & Bahndral, A. Kanthi Naveen, A. Probiotics- its functions and influence on the ageing process: A comprehensive review. *Food Biosci.* **52**, 102389 (2023).
28. Ghosh, T. S., Shanahan, F. & O'Toole, P. W. The gut Microbiome as a modulator of healthy ageing. *Nat Rev. Gastroenterol. Hepatol.* **0123456789**, 565–584 (2022).
29. Sovran, B. et al. Age-associated impairment of the mucus barrier function is associated with profound changes in microbiota and immunity. *Sci. Rep.* **9**, 1437 (2019).
30. Sang, X. et al. Age-Related mucus barrier dysfunction in mice is related to the changes in Muc2 mucin in the colon. *Nutrients*. **15**, 1830 (2023).
31. Hii, H. P. et al. Improvement in heat stress-induced multiple organ dysfunction and intestinal damage through protection of intestinal goblet cells from prostaglandin E1 analogue Misoprostol. *Life Sci.* **310**, 121039 (2022).
32. Biagi, E. et al. Through ageing, and beyond: gut microbiota and inflammatory status in seniors and centenarians. *PLoS One*. **5**, e10667 (2010).
33. Dunlop, S. P., Jenkins, D. & Spiller, R. C. Age-related decline in rectal mucosal lymphocytes and mast cells. *Eur. J. Gastroenterol. Hepatol.* **16**, 1011–1015 (2004).
34. Kutukova, N. A., Nazarov, P. G. & Kudryavtseva, G. V. Shishkin, V. I. Mast cells and aging. *Adv. Gerontol. = Uspekhi Gerontol.* **29**, 586–593 (2016).
35. Grizzi, F. et al. Mast cells and the liver aging process. *Immun. Ageing*. **10**, 9 (2013).
36. Drozdowski, L. & Thomson, A. B. R. Aging and the intestine. *World J. Gastroenterol.* **12**, 7578–7584 (2006).
37. Buford, T. W. Dis)Trust your gut: the gut Microbiome in age-related inflammation, health, and disease. *Microbiome* **5**, 80 (2017).
38. Ceylani, T. & Teker, H. T. The effect of young blood plasma administration on gut microbiota in middle-aged rats. *Arch. Microbiol.* **204**, 541 (2022).
39. Indiani, C. M. D. S. P. et al. Childhood obesity and Firmicutes/Bacteroidetes ratio in the gut microbiota: A systematic review. *Child. Obes.* **14**, 501–509 (2018).
40. Li, G. et al. Intermittent fasting promotes white adipose Browning and decreases obesity by shaping the gut microbiota. *Cell. Metab.* **26**, 672–685e4 (2017).
41. Xu, Y., Zhu, Y., Li, X. & Sun, B. Dynamic balancing of intestinal short-chain fatty acids: the crucial role of bacterial metabolism. *Trends Food Sci. Technol.* **100**, 118–130 (2020).
42. Ardahanlı, İ. et al. Infrared spectrochemical findings on intermittent fasting-associated gross molecular modifications in rat myocardium. *Biophys. Chem.* **289**, 106873 (2022).
43. Gurbanov, R., Kabaoğlu, U. & Yağcı, T. Metagenomic analysis of intestinal microbiota in wild rats living in urban and rural habitats. *Folia Microbiol. (Praha)*. **67**, 469–477 (2022).
44. Yang, T. et al. Gut dysbiosis is linked to hypertension. *Hypertension* **65**, 1331–1340 (2015).
45. Altintas, T. et al. Targeting gut microbiota health in aged rats through the potent strategy of probiotics supplementation during intermittent fasting. *Pak Vet. J.* **45**, 286–294 (2025).
46. Ceylani, T., Taner, H., Samgane, G. & Gurbanov, R. Intermittent fasting-induced biomolecular modifications in rat tissues detected by ATR-FTIR spectroscopy and machine learning algorithms. *Anal. Biochem.* **654**, 114825 (2022).
47. Baba, B. et al. Promoting longevity in aged liver through NLRP3 inflammasome Inhibition using Tauroursodeoxycholic acid (TUDCA) and SCD probiotics. *Arch. Gerontol. Geriatr.* **125**, 105517 (2024).
48. Keskin, S., Acikgoz, E., Ertürk, F. Y., Ragbetli, M. C. & Ozkol, H. Histopathological changes in liver and heart tissue associated with experimental ultraviolet radiation A and B exposure on Wistar albino rats. *Photochem. Photobiol.* **99**, 132–136 (2023).
49. Ceylani, T., Önlü, H., Keskin, S., Allahverdi, H. & Teker, H. T. SCD probiotics mitigate cafeteria diet-induced liver damage in Wistar rats during development. *J. Gastroenterol. Hepatol.* **38**, 2142–2151 (2023).

50. Adomshick, V., Pu, Y. & Veiga-Lopez, A. Automated lipid droplet quantification system for phenotypic analysis of adipocytes using cellprofiler. *Toxicol. Mech. Methods.* **30**, 378–387 (2020).

Acknowledgements
We would like to thank Adem Kurtcuoğlu for his contributions.

Author contributions
TC, HTT: Conceptualization, Data curation, Formal analysis, Funding acquisition, Investigation, Methodology, Resources, Software, Supervision, Validation, Visualization, Writing – original draft, Writing – review & editing. EA, SK: Formal analysis, Methodology, Resources, Supervision, Validation, Visualization, Writing – original draft, Review & Editing.ES, MT: Formal analysis, Methodology, Supervision, Validation, Writing – original draft, Review & Editing.RG: Data curationFormal analysis, Methodology, Resources, Supervision, Validation, Visualization, Writing – original draft, Review & Editing.

Funding
This research received no specific grant from any funding agency in the public, commercial, or not-for-profit sectors.

Declarations

Competing interests
The authors declare no competing interests.

Ethics approval
This study was carried out with the approval of the Ethics Committee (meeting date: 05/03/2021, approval number: 2021/05) from the Saki Yenilli Experimental Animal Production and Practice Laboratory.

Additional information
Supplementary Information The online version contains supplementary material available at https://doi.org/10.1038/s41598-025-21183-3.

Correspondence and requests for materials should be addressed to T.C. or H.T.T.

Reprints and permissions information is available at www.nature.com/reprints.

Publisher's note Springer Nature remains neutral with regard to jurisdictional claims in published maps and institutional affiliations.